Acid-Induced Unfolding Mechanism of Recombinant Human Endostatin†

Bing Li, Xiaoyu Wu, Hao Zhou, Qianjie Chen,‡ and Yongzhang Luo*

Department of Biological Sciences and Biotechnology, MOE laboratory of Protein Science, Tsinghua University, Beijing 100084, P. R. China

Received October 3, 2003; Revised Manuscript Received December 9, 2003

ABSTRACT: Endostatin is a potent angiogenesis inhibitor. The structure of endostatin is unique in that its secondary structure is mainly irregular loops and β-sheets and contains only a small fraction of α-helices with two pairs of disulfide bonds in a nested pattern. We choose human endostatin as a model system to study the folding mechanism of this kind. Nuclear magnetic resonance (NMR), tryptophan emission fluorescence, and circular dichroism (CD) were used to monitor the unfolding process of endostatin upon acid titration. Urea-induced unfolding was used to measure the stability of endostatin under different conditions. Our results show that endostatin is very acid-resistant; some native structure still remains even at pH 2 as evidenced by ^{1}H NMR. Trifluoroethanol (TFE) destabilizes native endostatin, while it makes endostatin even more acid-resistant in the low pH region. Stability measurement of endostatin suggests that endostatin is still in native structure at pH 3.5 despite the decreased stability. Acid-induced unfolding of endostatin is reversible, although it requires a long time to reach equilibrium below pH 3. Surprisingly, the α-helical content of endostatin is increased when it is unfolded at pH 1.6, and the α-helical content of the polypeptide chain of unfolded endostatin increases linearly with TFE concentration in the range of 0−30%. This observation indicates that the polypeptide chain of unfolded endostatin has an intrinsic α-helical propensity. Our discoveries may provide clues for refolding endostatin more efficiently. The acid-resistance property of endostatin may have biological significance in that it cannot be easily digested by proteases in an acidic environment such as in a lysosome in the cell.

Endostatin, a 20 kD C-terminal fragment of collagen XVIII, can specifically inhibit endothelial cell proliferation and thus potently inhibit angiogenesis and tumor growth (*1*−*3*) without induced toxicity and acquired drug resistance (*2*). Inducing apoptosis of endothelial cells (*1*, *4*) is thought to be critical for the antiangiogenesis property of endostatin. The crystal structure of endostatin reveals a compact fold (*5*, *6*): its secondary structure includes predominantly β-sheets and loops; there are also two α-helices, and one of them is short. The fold of endostatin is intricate: the most prominent property is a highly twisted mixed β-sheet with 14 residues containing α-helix packing against one face of the sheet. A zinc ion is bound near its N-terminus (*5*). Endostatin contains two pairs of disulfide bonds in a unique nested form (*5*, *6*). Although there have been many reports on the antitumor activity (*2*, *7*) and clinical trials of endostatin in recent years (*8*), there has been no paper reported on the physical and chemical properties of this protein except Chung and his colleagues who reported the circular dichroism spectrum of endostatin (*9*). There is no report so far about the folding mechanism of endostatin.

Acid can induce the formation of folding intermediates or molten globules of many proteins (*10*), including apomyoglobin (*11*, *12*), α-lactalbumin (*13*, *14*), and β-lactoglobulin (*15*), and similar molten globules can also occur on the kinetic folding pathway (*16*). The intermediates can be either marginally stable, highly disordered conformations or stable states with nearly native structures (*17*−*25*), while they share the same properties, a significant amount of secondary structure and fluctuating tertiary structure (if any) with partially exposed hydrophobic surfaces. We are interested in knowing the behavior of endostatin in different acidic conditions and want to test whether a folding intermediate or molten globule is formed under these conditions. Classical model proteins used for studying protein folding mechanisms as mentioned above rarely contain disulfide bridges in the kind of complex nested pattern like endostatin, we therefore choose endostatin, an angiogenesis inhibitor, as a model system for studying the folding mechanism of this kind. Moreover, expression of human endostatin in yeast has low expression yield with low recovery during purification (*26*), while refolding of inclusion bodies of endostatin expressed in *Escherichia coli* failed to give satisfactory recovery yield (*1*) due to its complicated tertiary structure, which is a serious problem in the pharmaceutical industry. Understanding the folding mechanism of endostatin may be very important for producing a large amount of refolded endostatin from inclusion bodies.

† Supported in part by grants from National Science Foundation for Outstanding Young Scientists in China (No. 30225014), the Key Program of National Science Foundation (No. 30291000), National 863 Program of China (No. 2001AA215041, 2002AA2Z345D, and No. 2002AA2Z3328), Science & Technology Research Project of the Ministry of Education of China (No. 03007), and the 985 Project of Tsinghua University.

* To whom correspondence should be addressed. Tel: 010-6277-2897. Fax: 010-6279-4691. E-mail: protein@tsinghua.edu.cn.

‡ Present address: Medgenn Ltd., 1 Rongchang Road, Yantai Economy & Technology Development Zone, Yantai 264006, Shandong Province, P. R. China

10.1021/bi0357863 CCC: $27.50
Published on Web 02/13/2004

Endostatin is a very tight globular protein. Four tryptophans are buried in native endostatin, and their locations are relatively evenly distributed, which makes tryptophan emission fluorescence a good probe for detecting changes of tertiary structure upon acid titration or any other denaturant-induced unfolding (*27*, *28*). Our studies are designed to (1) test the behavior of endostatin in acidic conditions and measure acid stability of endostatin and (2) study the folding properties of endostatin under different acidic conditions. Several biophysical tools such as NMR, tryptophan emission fluorescence, and circular dichroism are used in the current study. What we found here is that endostatin is very acid-resistant; it still contains some native structure even at pH 2 as demonstrated by ^{1}H NMR measurements, and the presence of 5% 2,2,2-trifluoroethanol (TFE)[1] makes this protein even more acid-resistant in the low pH region. Stability measurements of endostatin by urea suggest that endostatin is still in the native structure at pH 3.5 despite the decreased stability. Interestingly, the α-helical content of endostatin is increased when it is unfolded at pH 1.6, and the presence of TFE can increase the α-helical content significantly. These observations indicate that the polypeptide chain of endostatin has an intrinsic propensity of forming α-helical structure. To our knowledge, this is the first report on the physical and chemical properties of endostatin regarding acid-induced unfolding.

MATERIALS AND METHODS

Materials. Urea, ultrapure 2,2,2-trifluoroethanol (TFE), and 1,4-dithiothreitol (DTT) were purchased from Sigma. Analytical grade acetic acid, sodium acetate, and hydrochloride acid (HCl) were purchased from Beijing Yili Corporation. The *E. coli* expressed recombinant human endostatin with MGGSHHHHH attached at the N-terminus was a gift from Medgenn Ltd. The purity of refolded endostatin was greater than 99% based on high performance liquid chromatography (HPLC) analysis. The activity of refolded endostatin was analyzed and verified on the basis of the endothelial cell proliferation and migration assays as described (*29*). Protein concentration was determined according to Edelhoch's method (*30*). All the proteins used in this study were free of zinc based on atomic absorption spectrometry.

pH Titration. Endostatin was first dissolved in 30 mM acetate (pH 5.5) to make a stock solution, which was diluted by aliquots into 4 mM acetate buffer at different pH values, using 1 M HCl to adjust pH when pH values were lower than 3.5. The final protein concentration was 0.6 μM. Tryptophan emission fluorescence, circular dichroism, or NMR measurements were carried out immediately after the samples were incubated at 20 °C for 100 min. However, the incubation time was reduced to 30 min in the presence of 5% TFE because of the faster equilibration process.

Urea-Induced Unfolding and Data Analysis. A stock solution of endostatin was diluted by aliquots into urea of different concentrations with a final protein concentration of 0.5 μM. The buffer was 5 mM Tris-HCl at pH 7.4 (with or without 5% TFE) or 4 mM sodium acetate at pH 3.5 (with or without 5% TFE). After incubation at 20 °C for 120 min (pH 7.4) or 60 min (pH 3.5), FL measurements were carried out.

Unfolding curves were analyzed by a two-state equation with linear baselines, according to the procedure of Santoro and Bolen (*31*) that uses data inside as well as outside the transition zone to fix the baselines. The native baselines for unfolding curves at pH 3.5 are fixed to the values of 0 M urea (with the slope of zero), because of the marginal stability and the difficulties in finding their baselines.

Tryptophan Emission Fluorescence Measurements. Tryptophan emission fluorescence measurements were carried out using an F-4500 fluorescence spectrophotometer (Hitachi) with a cuvette of 1 cm light path. The excitation wavelength at 288 nm was chosen because endostatin contains four tryptophan residues and excitation at 288 nm ensures fluorescence emission was mainly contributed by tryptophan residues. The tryptophan emission fluorescence spectra were collected between 295 and 400 nm. The slit widths for excitation and emission were 5 and 10 nm, respectively. The scan speed was 240 nm/min. All data were collected at 20 °C.

Hydrogen Exchange and ^{1}H NMR Measurements. One hundred sixty-six micromolar (166 μM) endostatin was dissolved in 10% D_2O in the presence of 4 mM acetate, incubated at 40 °C for 12 h to ensure complete H/D exchange of all solvent-accessible protons, and then lyophilized. The lyophilized protein was redissolved into D_2O to get the final protein concentration of 166 μM, using DCl and NaOD to adjust pH. Alternatively, endostatin samples were dissolved in a solution containing 16% D_2O and 4 mM acetate (with or without 5% TFE) with the final endostatin concentration of 166 μM. The samples were then incubated at 20 °C for 100 min before NMR measurement. ^{1}H NMR spectroscopy was taken at 500 MHz on a Varian Inova 500NB instrument. NMR spectra were acquired using a spectral width of 8000.0 Hz, a relaxation delay of 1.0 s, and 128 repetitions.

Secondary Structure Analysis. Circular dichroism measurements were performed on a Jasco-715 spectropolarimeter employing a 1 cm light path cuvette. The samples were treated the same as those in FL measurements except that the protein concentration was 2.3 μM. All data were collected at 20 °C. When the intrinsic α-helical propensity of the acid-unfolded state was examined, endostatin was dissolved into the buffer at pH 1.6 containing different concentrations of TFE (0, 5%, 10%, 20%, and 30%), and then the pH was checked; after about 100 min incubation at 20 °C, CD measurements were carried out.

RESULTS

Acid-Induced Unfolding Shows That Endostatin Is Acid-Resistant. Endostatin contains four tryptophan residues (W82, W114, W120, and W138) located evenly in space with all of their side chains stretching inside the molecule (*6*). We used tryptophan emission fluorescence to monitor the pH titration process of this protein. The tryptophan fluorescence emission spectrum of endostatin shows that its maximal emission wavelength is at 318 nm when excited at 288 nm under pH 6.4 (Figure 1A), which implies that native endostatin has a very tight tertiary structure. We thus monitor the pH titration process of endostatin using the tryptophan

[1] Abbreviations: FL, fluorescence; CD, circular dichroism; NMR, nuclear magnetic resonance; TFE, 2,2,2-trifluoroethanol; DTT, 1,4-dithiothreitol; ANS, 1-anilino-8-naphthalene sulfonate.

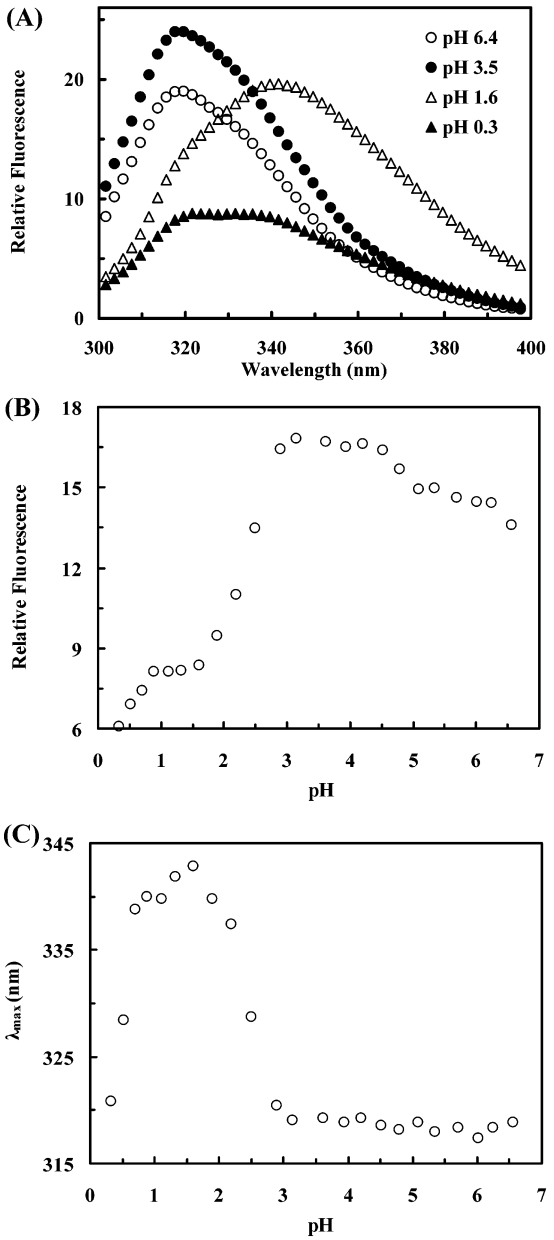

FIGURE 1: Acid-induced unfolding of endostatin monitored by tryptophan emission fluorescence: (A) tryptophan fluorescence emission spectra of endostatin at different pH; (B) relative fluorescence intensity monitored at 318 nm; (C) maximal emission wavelength (λ_{max}). The buffer was 4 mM sodium acetate, and the excitation wavelength was 288 nm. All measurements were carried out at 20 °C.

fluorescence emission intensity at 318 nm as shown in Figure 1B. It appears from this curve that an intermediate is formed between pH 4.5 and 3. However, the maximal emission wavelength of this intermediate is identical to that of the native state (N), that is, no red shift occurs (Figure 1C). The tryptophan fluorescence emission spectra are identical between pH 3 and 4.5, and they are also similar to that of the native state (pH 6.4) despite some increased intensity (Figure 1A). This indicates that endostatin still retains a very tight tertiary structure even at pH 3.

Endostatin starts to unfold around pH 3 (Figure 1B,C), and at pH 1.6, it is unfolded to the largest extent by acid (Figure 1C). This state is not completely unfolded because the maximal emission wavelength is 342 nm (Figure 1C) while other denaturants such as urea can unfold endostatin to have a maximal emission wavelength around 348 nm (see Figure 5 below).

When pH is decreased beyond pH 1.6, endostatin seems to refold again. Figure 1C shows that at pH 0.3 the maximal emission wavelength of endostatin is blue-shifted back to 320 nm indicating that the tryptophan residues are buried again. Although blue shift occurs at extreme acidic conditions, the tryptophan fluorescence emission intensity is decreased significantly (Figure 1B), which is consistent with an unfolded endostatin. The reason for the blue shifts of the maximal tryptophan fluorescence emission wavelengths at pH values lower than 1.6 is probably the anion effect (*24*, *32*) (here it is Cl^-), which shields the positive charges on endostatin so that the tryptophan residues are possibly buried in some hydrophobic clusters.

To verify that the "intermediate" state (between pH 4.5 and 3, Figure 1A) still retains native structure, NMR was employed to have a more precise detection. In the ^1H NMR spectra, the upfield chemical shifting of methyl peaks, the chemical shift dispersions in the aromatic region, and spreading out of the histidine $^1H^{\epsilon 1}$ resonances are all characteristic properties of tightly packed native proteins (*17*, *33*), all three of these characters are present in the NMR spectra of endostatin (taken in 16% D_2O) between pH values of 6.7 and 3. Although some interferences from backbone NH are present (Figure 2A), these interferences can be eliminated by taking the NMR spectra in 100% D_2O as shown in Figure 2B. The dispersion of the aromatic region becomes broader at lower pH indicating that the structure of endostatin fluctuates under these conditions; nevertheless, endostatin is still in the native state at pH 3 or above. We therefore conclude that the so-called "intermediate" state is still a native state but with some loose tertiary structure. The similar cooperativity in urea-induced unfolding of both the native (pH 7.4) and pH 3.5 state of endostatin also supports this conclusion (see Figure 5B below). It is obvious that some upfield chemical shifts of methyl groups still occur at pH 2, indicating some residual tertiary structure still remains, which may be localized around the disulfide bonds. Alternatively, it is possible that this state is a mixture of unfolded and folded states. No tertiary structure is detected at pH 1.6, an extremely low pH value for protein unfolding studies, based on NMR spectral analysis (Figure 2).

In sum, endostatin is very acid-resistant. There should be at least one or several acidic amino acid residues that have extremely low pK_a values in the native conformation (*34*) of endostatin. An alternative explanation cannot be excluded: that is, the unique nested cysteine structure makes endostatin so tightly packed (*5*, *6*) that it becomes acid-resistant.

Kinetic Study Shows That Acid-Induced Unfolding of Endostatin Is a Slow Process. Kinetic studies show that although acid-induced unfolding of endostatin reaches the equilibrium state within a few minutes above pH 3, the unfolding process becomes very slow below pH 3; for example, it requires about 90 min to reach the equilibrium state around pH 2 (Table 1), unlike many other proteins, which need only about a few minutes to reach their equilibrium (*11*−*15*). Interestingly, the slow process of acid-induced unfolding (Table 1) coincides with the equilibrium unfolding process as described in Figure 1B,C, which shows that acid-induced unfolding of endostatin starts around pH

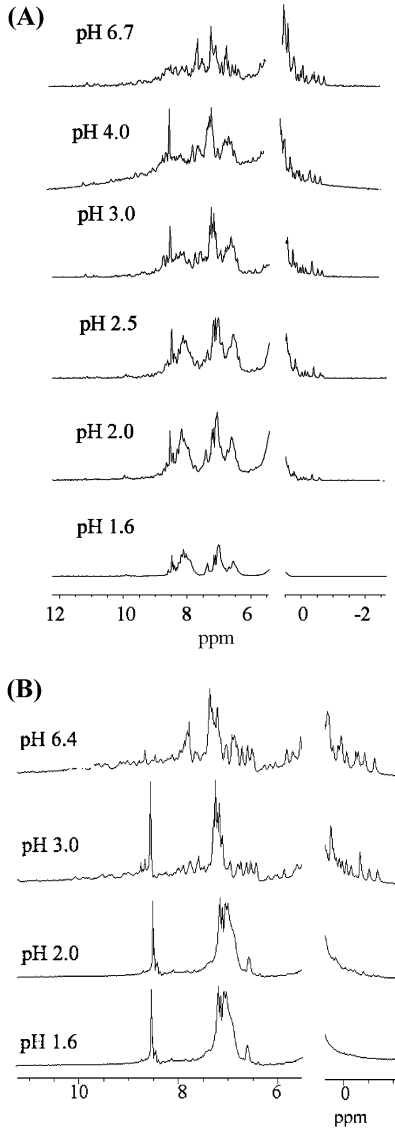

FIGURE 2: ^{1}H NMR spectra of endostatin at pH values between 1.6 and 6.7 collected in 16% D_2O (A) or 100% D_2O (B). The concentration of endostatin was 166 μM in 4 mM sodium acetate at 20 °C.

Table 1: Kinetics of Acid-Induced Unfolding of Endostatin[a]

pH	λ_{max} (nm)[b]	t_{eq} (min)[c]
6.4	318	<1
6.4−2.9	318−320	<10
2.4	~325	~80
2.0	~337	~90
1.6	~342	~80
0.3−0.4	~320	~6

[a] The reactions were carried out in 4 mM sodium acetate at 20 °C. [b] λ_{max}, maximal emission wavelength. [c] t_{eq}, the time needed to reach equilibrium at different pH.

3 and reaches the maximal unfolding around pH 1.6 (Figure 1C). Actually, unfolding processes of endostatin by urea are also very slow (data not shown); about 100 min enables endostatin to be completely denatured in high concentration of urea. The kinetic studies indicate that there is possibly a large kinetic barrier between native and unfolded endostatin in the unfolding pathway.

Effect of TFE on the Stability of Endostatin at Neutral and Acidic pH. It has been reported by Luo and Baldwin

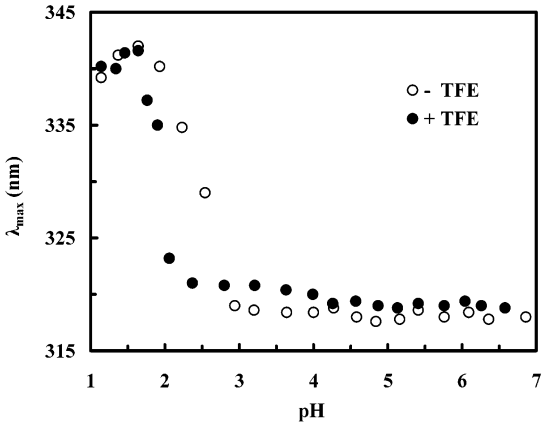

FIGURE 3: Acid-induced unfolding of endostatin in the presence of 5% TFE monitored by fluorescence maximal emission wavelength. The buffer was 4 mM sodium acetate containing 5% TFE, and the excitation wavelength was 288 nm. All measurements were carried out at 20 °C.

(*35*) that TFE stabilizes the pH 4 folding intermediate of apomyoglobin while it destabilizes the native structures of holomyoglobin, lysozyme, and RNase A. We thus tested whether TFE has a similar effect on endostatin; especially, we want to know whether the pH 3.5 state more closely mimics a folding intermediate or a native state. The pH-titration curve of endostatin in the presence of 5% TFE is shown in Figure 3. TFE slightly destabilizes the native structure of endostatin between pH 3 and 7 as evidenced by the red shift of the maximal tryptophan fluorescence emission wavelength (Figure 3). This observation once again is consistent with our earlier conclusion that endostatin still retains native structure even at pH 3 (see Figure 1).

Surprisingly, TFE stabilizes endostatin between pH 3 and 1.5. Unlike in the absence of TFE where endostatin starts to unfold at pH 3, endostatin starts to unfold at about pH 2.4 in the presence of 5% TFE (Figure 3). Therefore, TFE makes endostatin more acid-resistant in the low pH region. Results from ^{1}H NMR measurements are also consistent with this conclusion as shown in Figure 4. That TFE makes endostatin more acid-resistant can be explained by the fact that TFE stabilizes secondary structure of proteins by strengthening the hydrogen bonds of proteins (*36*).

To test the effect of TFE on the stability of endostatin at both neutral and acidic pH, urea-induced unfolding at pH 7.4 and pH 3.5, with or without TFE (Figure 5) was carried out. Evidently TFE destabilizes endostatin both at pH 7.4 and pH 3.5 even at as low as 5% TFE (Figure 5A, Table 2). By normalization of the raw data according to the method of Santoro and Bolen (*31*) as shown in Figure 5B, the unfolding curves at pH 7.4 and pH 3.5 in the absence of TFE have similar m^* values despite the decrease in the C_m values from 3.58 to 1.52 M (Table 2). Since the m^* value is a measure of folding cooperativity, the similar m^* values at both pH 7.4 and 3.5 strongly suggest that endostatin is not in the intermediate state but rather still retains native structures at pH 3.5. TFE has a stronger effect on decreasing both the stability and cooperativity of endostatin at pH 3.5 than at pH 7.4. Five percent TFE decreases the C_m value by 0.47 M at pH 3.5, while it decreases the C_m value by only 0.33 M at pH 7.4 (Figure 5B and Table 2), suggesting that although endostatin still retains native structure at pH 3.5, this state is less stable than the pH 7.4 state. Five percent

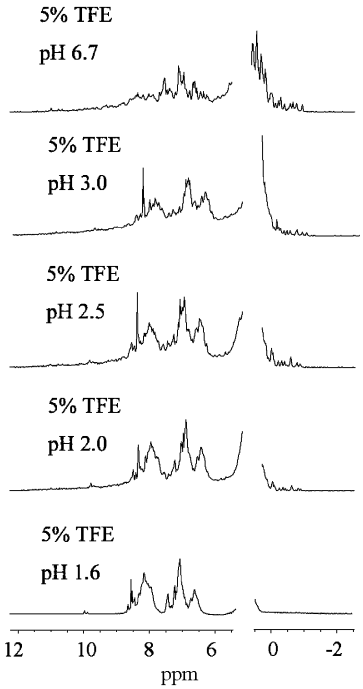

FIGURE 4: Acid-induced unfolding of endostatin in the presence of 5% TFE monitored by ^{1}H NMR. Sample conditions were 166 μM endostatin in 4 mM sodium acetate containing 5% TFE at 20 °C.

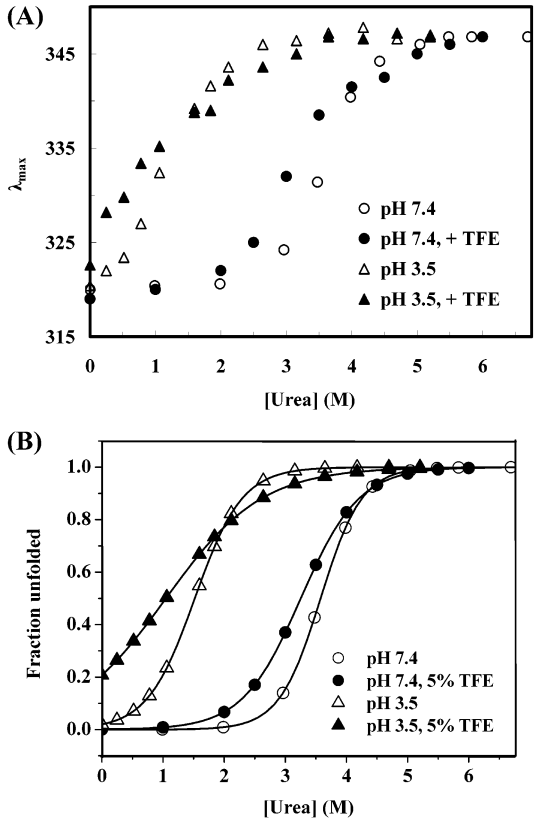

FIGURE 5: Stability measurements of endostatin in urea under neutral and acidic conditions. The buffer was 5 mM Tris-HCl (pH 7.4) or 4 mM acetate (pH 3.5) with or without 5% TFE: (A) raw data; (B) normalized data. The excitation wavelength was 288 nm. All measurements were performed at 20 °C.

TFE decreases the *m** values of endostatin by more than 50% at pH 3.5, while it decreases by only less than 30% the *m** values at pH 7.4 (Table 2). The stronger effect of 5% TFE in decreasing the *m** values of endostatin at pH 3.5 results in a much less cooperative unfolding induced by urea (Figure 5B).

Table 2: Parameters of Urea-Unfolding Curves[a]

conditions	C_m[b]	*m** (cal·mol^{-1}·M^{-1})[c]
pH 7.4	3.58	1758
pH 7.4, 5% TFE	3.25	1246
pH 3.5	1.52	1528
pH 3.5, 5% TFE	1.05	757

[a] The experiments were carried out in 5 mM Tris-HCl at pH 7.4 (with or without 5% TFE) or 4 mM sodium acetate at pH 3.5 (with or without 5% TFE) at 20 °C. [b] C_m, the urea molarity at the midpoint of the unfolding transition. [c] *m**, the apparent *m* value defined by the linear extrapolation model.

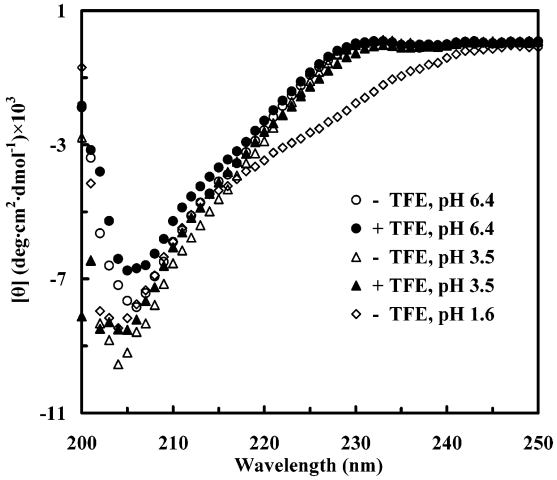

FIGURE 6: Circular dichroism spectra of endostatin at different pH with or without 5% TFE. [θ] represents mean residue ellipticity. Endostatin concentration was 2.3 μM. All measurements were carried out at 20 °C.

Unfolding of Endostatin Is Reversible. When the pH was raised directly from pH 1.6, the most unfolded state of endostatin, to pH 6.0, a typical tryptophan fluorescence emission spectrum of native endostatin was observed (data not shown). Moreover, the refolding curve by neutralizing the pH 1.6 unfolded endostatin is in superimposition to that of the acid-induced unfolding curve. These observations suggest that the acid-induced unfolding of endostatin is reversible. The refolding process from the pH 1.6 unfolded endostatin to native endostatin requires about 27 min, while that of the unfolding process requires about 90 min at pH values below 3, that is, the process of refolding is faster than that of unfolding.

Unfolded Endostatin Has a High Helical Content. The secondary structure of endostatin contains a large fraction of irregular loop structures and β-sheets and a small fraction of α-helices (*5*, *6*), which suggests that circular dichroism (CD) may not be a sensitive probe to monitor the changes in the helical content of endostatin upon acid-induced unfolding. This prediction is verified in Figure 6 where no significant difference in the helical content is detected between pH 3.5 and 6.4, while there is an increase in tryptophan fluorescence emission intensity (Figure 1). Surprisingly, there is an increase in the amount of α-helical content when endostatin is unfolded at pH 1.6 (Figure 6), which suggests that the unfolded endostatin may have an intrinsic helical propensity. Since TFE can destroy tertiary

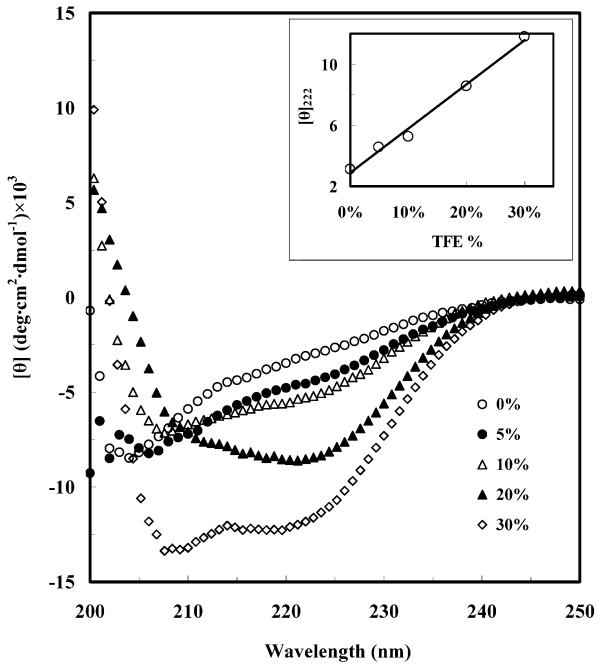

FIGURE 7: Effect of TFE on the secondary structure of acid-unfolded endostatin at pH 1.6. [θ] represents mean residue ellipticity. The inset shows the dependence of α-helical content on TFE concentration, $[\theta]_{222}$ represents mean residue ellipticity at 222 nm; the unit for $[\theta]_{222}$ is (deg·cm^2·dmol^{-1}) × 10^3. All samples were at pH 1.6 containing different concentrations of TFE as indicated. All measurements were carried out at 20 °C.

structure (*35*) while it can increase α-helical structure of proteins and peptides (*36*, *37*), we thus tested the behavior of TFE on the amount of α-helical content of endostatin at different pH values. We are especially interested in seeing whether TFE can further increase the α-helical structure of endostatin at pH 1.6. Since helical propensities of polypeptides increase linearly with TFE concentration in the range of 0−30% (*38*), we therefore tested a range of TFE concentration (<30%) on the helical content of endostatin at pH 1.6. Indeed, the α-helical structure of endostatin increases linearly with TFE concentration between 0 and 30% at pH 1.6 (Figure 7), which once again confirms that the polypeptide chain of endostatin has an intrinsic α-helical propensity in the unfolded state at pH 1.6. Although 5% TFE has a strong impact on the secondary structure of unfolded endostatin (Figure 7), it has limited effect on the native state (Figure 6), which probably reflects the fact that both the tightly packed tertiary structure and the stabilizing effect of TFE on the secondary structure override the destabilizing effect of TFE on the tertiary structure of native endostatin.

DISCUSSION

Contribution of Acidic Amino Acid Residues to the Acid-Induced Unfolding of Endostatin. Endostatin contains a large number of charged residues: 15 negatively charged groups (aspartate and glutamate), 20 positively charged groups (arginine and lysine), and 7 histidine residues. Most of these charged groups are located on the surface, while few of them are relatively less accessible to water and proton (*5*, *6*). His121 is the only histidine residue that is completely buried inside the hydrophobic core of native endostatin, which may endow His121 with a pK_a value much lower than 6.5, the normal pK_a value for the side chain of histidine residue (*34*). Therefore, it is likely that protonation of His121 at pH 5 may trigger the loosening of the native structure of endostatin (Figure 1).

The turn point of acid-induced unfolding occurs around pH 3, while it is shifted to around pH 2.4 when 5% TFE is present (Figure 3). These two pH values are significantly lower than the normal pK_a values of 4.3 and 3.9 for the side chains of aspartate and glutamate, respectively (*39*, *40*). It is therefore possible that there is at least one amino acid residue that has an unusually low pK_a value (*34*); protonation of such a residue causes unfolding of endostatin. Site-directed mutagenesis can be used to probe whether His121 and some other acidic groups play important roles in the acid-induced unfolding of endostatin.

No Equilibrium Intermediate Exists under Acidic Conditions. TFE has a "double edged" effect on proteins and peptides: on one hand, it stabilizes the helical structure of proteins and peptides by strengthening the hydrogen bonds (*36*); on the other hand, it destroys the tertiary structure of proteins by weakening the hydrophobic interactions (*35*, *41*). The observation that 5% TFE weakens the tertiary structure of endostatin between pH 7 and 3 while it makes endostatin more acid-resistant in the low pH region (shifting the turn point of unfolding from 3 to 2.4) (Figure 3) suggests that strengthening the hydrogen bonds by TFE plays the dominant role to make endostatin more resistant to acid. Five percent TFE decreases the stability of endostatin both at pH 7.4 and at pH 3.5 (Figure 5 and Table 2); this may indicate that no equilibrium intermediate exists under acidic conditions since a low concentration of TFE should stabilize an intermediate (*35*).

Although two-dimensional NMR can be a powerful tool in resolving the structural details of proteins, resolving a 2D NMR spectrum with a protein as big as endostatin at a molecular weight of 21 kD would be quite difficult, especially under acidic conditions. The difficulty comes from the line broadening resulting from the conformational exchange in loosely packed endostatin at acidic conditions such as at pH 2.

Although 1-anilino-8-naphthalene sulfonate (ANS) has been used extensively in probing protein folding intermediates, contradictory observations have been reported. Ptitsyn and his colleagues used ANS as a hydrophobic fluorescent probe in studying the kinetics of refolding of bovine carbonic anhydrase B (*42*). However, Bhakuni and his colleagues reported that ANS can induce molten globule formation from acid-unfolded cytochrome *c* (*43*); Kamen and Woody reported that addition of ANS to acid-denatured pectate lyase C leads to the formation of a partially folded intermediate (*44*); Matulis and his colleagues reported that bovine serum albumin and γ-globulin, starting from their acid-expanded, most hydrated conformations, undergo extensive molecular compaction upon ANS binding (*45*). All these studies indicate that ANS can induce protein conformational change. Therefore, ANS is not always a definitive reporter of protein conformations existing before ANS binding, especially at acidic conditions. That was the reason ANS was not used in the current study.

Intrinsic α-Helical Propensity of the Polypeptide Chain of Endostatin. The observation that unfolded endostatin at pH 1.6 has a higher α-helical content than the native state is very interesting (Figure 6). One explanation is that the

polypeptide chain of endostatin has an intrinsic α-helical propensity; addition of TFE should increase the α-helical content of this polypeptide. Indeed, TFE greatly increases the α-helical content of the unfolded endostatin, obviously leading to some nonnative α-helical structure formation, and the α-helical content of endostatin at pH 1.6 is nearly linearly dependent on TFE concentration (Figure 7 and the inset). A similar conclusion has been reported by Goto and his colleagues on β-lactoglobulin (*46*), who observed that several fragments that adopt β-strand conformation in the native state of β-lactoglobulin in fact have high helical propensity. Goto and his colleagues therefore concluded (*46*, *47*) that the intrinsic helical propensity of a peptide is not necessarily related to the secondary structure in the native state, and it may suggest a case of a nonhierarchical protein folding model. Unlike apomyoglobin, which decreases in α-helical structure upon unfolding (*48*, *28*) because of its high α-helical content in the native state, endostatin shows the reverse effect upon unfolding: its acid-unfolded state has higher α-helical content compared with the native state. Dissecting endostatin into different fragments to find out which part has intrinsic helical propensity is currently under investigation.

Possible Roles of the Disulfide Bonds in the Acid-Resistant Property of Endostatin. Endostatin contains two pairs of disulfide bonds in a nested pattern (*6*); an alternative explanation to account for the acid-resistant property of endostatin is the contribution from the two pairs of unique disulfide bonds. We have observed that reduction of the two disulfide bonds is a slow process: it takes at least 6 h at room temperature to completely reduce them by 10 mM dithiothreitol (DTT) at pH 8.6 in the presence of 8 M urea, while endostatin cannot be completely reduced when denaturant is absent. Reduced endostatin is extremely insoluble in the absence of denaturant (data not shown), and this is why we did not carry out the acid-induced unfolding of endostatin in the reduced form. One explanation for the slow reduction of endostatin is that the two pairs of disulfide bonds are less accessible to DTT, a very powerful reducing agent for cystine. In fact, the two pairs of disulfide bonds (C33−C173 and C135−C165) hold endostatin so tightly that a very symmetrical sphere conformation is formed (6): C33−C173 links the longer α-helix (α1) with another inner β-strand (P), linking the two ends of endostatin together, while C135−C165 links the two carbonyl ends of another two β-strands (L and O) together. The tightly packed endostatin may render it acid-resistant, partly due to its lower accessibility to protons and partly due to its stable conformation. The less-accessible character may also account for the slow kinetics of unfolding and refolding of endostatin.

The unique nested pattern of disulfide bonds may also be responsible for the failure in forming a molten globule in the acid-induced unfolding pathway of endostatin. If it is indeed the case, a molten globule state may be induced when one or both of the two disulfide bonds are knocked out, just like α-lactalbumin, which forms a molten globule when its disulfide bonds are mutated (*49*, *50*). Such a hypothesis and the contribution of the two pairs of disulfide bonds to the stability of endostatin are under investigation.

Potential Applications and Biological Implications. Refolding of endostatin from inclusion bodies has been proved to be very difficult with a recovery of less than 1% at physiological conditions (*1*). Our study on the acid-induced unfolding mechanism of this protein provides clues for refolding of endostatin more efficiently at acidic conditions; for example, since endostatin contains native structure even at pH 2, refolding inclusion bodies of endostatin at acidic conditions may be an alternative way for obtaining large amount of native endostatin.

Endostatin can bind to several proteins both inside the endothelial cells such as tropomyosin (*51*) and on the surface of human endothelial cells such as integrins (*52*). Endostatin can also induce tyrosine kinase signaling through Shb adaptor protein (*53*). Internalization of endostatin by endothelial cells has been observed both by Dixelius and his colleagues (*53*) and us (to be submitted), which may imply an early phase in the antiangiogenesis functional mechanism of endostatin. The biological significance of the acid-resistance property of endostatin may line in that the internalized endostatin may remain so tightly packed in acidic environments such as in lysosomes, where the pH ranges from 4.5 to 5 (*54*), that it cannot be easily digested by proteases.

ACKNOWLEDGMENT

We gratefully acknowledge R. L. Baldwin and members of the Luo laboratory for insightful discussions and criticism throughout the course of this work, Medgenn Ltd. for cooperation in the preparation of endostatin sample, and Yongbin Yan for his assistance with the NMR facilities of the Department of Biological Sciences & Biotechnology at Tsinghua University.

REFERENCES

1. O'Reilly, M. S., Boehm, T., Shing, Y., Fukai, N., Vasios, G., Lane, W. S., Flynn, E., Birkhead, J. R., Olsen, B. R., and Folkman, J. (1997) Endostatin: an endogenous inhibitor of angiogenesis and tumor growth, *Cell 88*, 277−285.
2. Boehm, T., Folkman, J., Browder, T., and O'Reilly, M. S. (1997) Antiangiogenic therapy of experimental cancer does not induce acquired drug resistance, *Nature 390*, 404−407.
3. Yamaguchi, N., Anand-Apte, B., Lee, M., Sasaki, T., Fukai, N., Shapiro, R., Que, I., Lowik, C., Timpl, R., and Olsen, B. R. (1999) Endostatin inhibits VEGF-induced endothelial cell migration and tumor growth independently of zinc binding, *EMBO J. 18*, 4414−4423.
4. Dhanabal, M., Ramchandran, R., Waterman, M. J. F., Lu, H., Knebelmann, B., Segal, M., and Sukhatme, V. P. (1999) Endostatin induces endothelial cell apoptosis, *J. Biol. Chem. 274*, 11721−11726.
5. Ding, Y. H., Javaherian, K., Lo, K. M., Chopra, R., Boehm, T., Lanciotti, J., Harris, B. A., Li, Y., Shapiro, R., Hohenester, E., Timpl, R., Folkman, J., and Wiley, D. C. (1998) Zinc-dependent dimers observed in crystals of human endostatin, *Proc. Natl. Acad. Sci. U.S.A. 95*, 10443−10448.
6. Hohenester, E., Sasaki, T., Olsen, B. R., and Timpl, R. (1998) Crystal structure of the angiogenesis inhibitor endostatin at 1.5 Å resolution, *EMBO J. 17*, 1656−1664.
7. Black, W. R., and Agner, R. C. (1998) Tumour regression after endostatin therapy, *Nature 391*, 450.
8. Bachelot, T., Jouanneau, E., and Blay, J. Y. (2003) Clinical development of anti-angiogenic agents in 2002, *Bull. Cancer 90*, 19−23.
9. You, W. K., So, S. H., Lee, H., Park, S. Y., Yoon, M. R., Chang, S. I., Kim, H. K., Joe, Y. A., Hong, Y. K., and Chung, S. I. (1999) Purification and characterization of recombinant murine endostatin in *E. coli*, *Exp. Mol. Med. 31*, 197−202.
10. Fink, A. L., Calciano, L. J., Goto, Y., Kurotsu, T., and Palleros, D. R. (1994) Classification of acid denaturation of proteins: intermediates and unfolded states, *Biochemistry 33*, 12504−12511.

11. Hughson, F. M., Wright, P. E., and Baldwin, R. L. (1990) Structural characterization of a partly folded apomyoglobin intermediate, *Science 249*, 1544−1548.
12. Barrick, D., and Baldwin, R. L. (1993) Stein and Moore Award address. The molten globule intermediate of apomyoglobin and the process of protein folding, *Protein Sci. 2*, 869−876.
13. Kuwajima, K. (1996) The molten globule state of alpha-lactalbumin, *FASEB J. 10*, 102−109.
14. Luo, Y., and Baldwin, R. L. (1999) The 28-111 disulfide bond constrains the alpha-lactalbumin molten globule and weakens its cooperativity of folding, *Proc. Natl. Acad. Sci. U.S.A. 96*, 11283−11287.
15. Ptitsyn, O. B., Pain, R. H., Semisotnov, G. V., Zerovnik, E., and Razgulyaev, O. I. (1990) Evidence for a molten globule state as a general intermediate in protein folding, *FEBS Lett. 262*, 20−24.
16. Jennings, P. A., and Wright, P. E. (1993) Formation of a molten globule intermediate early in the kinetic folding pathway of apomyoglobin, *Science 262*, 892−896.
17. Loh, S. N., Kay, M. S., and Baldwin, R. L. (1995) Structure and stability of a second molten globule intermediate in the apomyoglobin folding pathway, *Proc. Natl. Acad. Sci. U.S.A. 92*, 5446−5450.
18. Ptitsyn, O. B. (1995) Molten globule and protein folding, *Adv. Protein Chem. 47*, 83−229.
19. Dobson, C. M. (1994) Protein folding. Solid evidence for molten globules, *Curr. Biol. 4*, 636−640.
20. Peng, Z. Y., Wu, L. C., Schulman, B. A., and Kim, P. S. (1995) Does the molten globule have a native-like tertiary fold? *Philos. Trans. R. Soc. London, Ser. B 348*, 43−47.
21. Lin, L., Pinker, R. J., Forde, K., Rose, G. D., and Kallenbach, N. R. (1994) Molten globular characteristics of the native state of apomyoglobin, *Nat. Struct. Biol. 1*, 447−452.
22. Chakraborty, S., and Peng, Z. Y. (2000) Hierarchical Unfolding of the α-Lactalbumin Molten Globule: Presence of a Compact Intermediate Without a Unique Tertiary Fold, *J. Mol. Biol. 298*, 1−6.
23. Wu, L. C., Peng, Z. Y., and Kim, P. S. (1995) Bipartite structure of the alpha-lactalbumin molten globule, *Nat. Struct. Biol. 2*, 281−286.
24. Goto, Y., Calciano, L. J., and Fink, A. L (1990) Acid-induced folding of proteins, *Proc. Natl. Acad. Sci. U.S.A. 87*, 573−577.
25. Englander, S. W. (2000) Protein folding intermediates and pathways studied by hydrogen exchange, *Annu. Rev. Biophys. Biomol. Struct. 29*, 213−238.
26. Dhanabal, M., Ramchandran, R., Volk, R., Stillman, I. E., Lombardo, M., Iruela-Arispe, M. L., Simons, M., and Sukhatme, V. P. (1999) Endostatin: yeast production, mutants, and antitumor effect in renal cell carcinoma, *Cancer Res. 59*, 189−197.
27. Kay, M. S., and Baldwin, R. L. (1996) Packing interactions in the apomyglobin folding intermediate, *Nat. Struct. Biol. 3*, 439−345.
28. Luo, Y., Kay, M. S., and Baldwin, R. L. (1997) Cooperativity of folding of the apomyoglobin pH 4 intermediate studied by glycine and proline mutations, *Nat. Struct. Biol. 4*, 925−930.
29. O'Reilly, M. S., Holmgren, L., Shing, Y., Chen, C., Rosenthal, R. A., Moses, M., Lane, W. S., Cao, Y., Sage, E. H., and Folkman, J. (1994) Angiostatin: a novel angiogenesis inhibitor that mediates the suppression of metastases by a Lewis lung carcinoma, *Cell 79*, 315−328.
30. Edelhoch, H. (1967) Spectroscopic determination of tryptophan and tyrosine in proteins, *Biochemistry 6*, 1948−1954.
31. Santoro, M. M., and Bolen, D. W. (1988) Unfolding free energy changes determined by the linear extrapolation method. 1. Unfolding of phenylmethanesulfonyl alpha-chymotrypsin using different denaturants, *Biochemistry 27*, 8063−8068.
32. Goto, Y., Takahashi, N., and Fink, A. L. (1990) Mechanism of acid-induced folding of proteins, *Biochemistry 29*, 3480−3488.
33. Redfield, C., and Dobson, C. M. (1988) Sequential ^{1}H NMR assignments and secondary structure of hen egg white lysozyme in solution, *Biochemistry 27*, 122−136.
34. Geierstanger, B., Jamin, M., Volkman, B. F., and Baldwin, R. L. (1998) Protonation behavior of histidine 24 and histidine 119 in forming the pH 4 folding intermediate of apomyoglobin, *Biochemistry 37*, 4254−4265.
35. Luo, Y., and Baldwin, R. L. (1998) Trifluoroethanol stabilizes the pH 4 folding intermediate of sperm whale apomyoglobin, *J. Mol. Biol. 279*, 49−57.
36. Luo, P., and Baldwin, R. L. (1997) Mechanism of helix induction by trifluoroethanol: a framework for extrapolating the helix-forming properties of peptides from trifluoroethanol/water mixtures back to water, *Biochemistry 36*, 8413−8421.
37. Cammer-Goodwin, A., Allen, T. J., Oslick, S. L., McClure, K. F., Lee, J. H., and Kemp, D. S. (1996) Mechanism of stabilization of helical conformations of polypeptides by water containing trifluoroethanol, *J. Am. Chem. Soc. 118*, 3082−3090.
38. Jasanoff, A., and Fersht, A. R. (1994) Quantitative Determination of Helical Propensities from Trifluoroethanol Titration Curves, *Biochemistry 33*, 2129−2135.
39. Nozaki, Y., and Tanford, C. (1967) Proteins as random coils. II. Hydrogen ion titration curve of ribonuclease in 6 M guanidine hydrochloride, *J. Am. Chem. Soc. 89*, 742−749.
40. Roxby, R., and Tanford, C. (1971) Hydrogen ion titration curve of lysozyme in 6 M guanidine hydrochloride, *Biochemistry 10*, 3348−3352.
41. Brandts, J. F., and Hunt, L. (1967) The thermodynamics of protein denaturation. 3. The denaturation of ribonuclease in water and in aqueous urea and aqueous ethanol mixtures, *J. Am. Chem. Soc. 89*, 4826−4838.
42. Semisotnov, G. V., Rodionova, N. A., Kutyshenko, V. P., Ebert, B., Blanck, J., and Ptitsyn, O. B. (1987) Sequential mechanism of refolding of carbonic anhydrase B, *FEBS Lett. 224*, 9−13.
43. Ali, V., Prakash, K., Kulkarni, S., Ahmad, A., Madhusudan, K. P., and Bhakuni, V. (1999) 8-Anilino-1-naphthalene sulfonic acid (ANS) induces folding of acid unfolded cytochrome *c* to molten globule state as a result of electrostatic interactions, *Biochemistry 38*, 13635−13642.
44. Kamen, D. E., and Woody, R. W. (2001) A partially folded intermediate conformation is induced in pectate lyase C by the addition of 8-anilino-1-naphthalenesulfonate (ANS), *Protein Sci. 10*, 2123−2130.
45. Matulis, D., Baumann, C. G., Bloomfield, V. A., and Lovrien, R. E. (1999) 1-Anilino-8-naphthalene sulfonate as a protein conformational tightening agent, *Biopolymers 49*, 451−458.
46. Hamada, D., Kuroda, Y., Tanaka, T., and Goto, Y. (1995) High helical propensity of the peptide fragments derived from β-lactoglobulin, a predominantly β-sheet protein, *J. Mol. Biol. 254*, 737−746.
47. Shiraki, K., Nishikawa, K., and Goto, Y. (1995) Trifluoroethanol-induced stabilization of the α-helical structure of β-lactoglobulin: Implication for non-hierarchical protein folding, *J. Mol. Biol. 245*, 180−194.
48. Luo, Y., and Baldwin, R. L. (2001) How Ala→Gly mutations in different helices affect the stability of the apomyoglobin molten globule, *Biochemistry 40*, 5283−5289.
49. Wu, L. C., Schulman, B. A., Peng, Z. Y., and Kim, P. S. (1996) Disulfide determinants of calcium-induced packing in α-lactalbumin, *Biochemistry 35*, 859−863.
50. Redfield, C., Schulman, B. A., Milhollen, M. A., Kim, P. S., and Dobson, C. M. (1999) Alpha-lactalbumin forms a compact molten globule in the absence of disulfide bonds, *Nat. Struct. Biol. 6*, 948−952.
51. MacDonald, N. J., Shivers, W. Y., Narum, D. L., Plum, S. M., Wingard, J. N., Fuhrmann, S. R., Liang, H., Holland-Linn, J., Chen. D. H., and Sim, B. K. (2001) Endostatin binds tropomyosin. A potential modulator of the antitumor activity of endostatin, *J. Biol. Chem. 276*, 25190−25196.
52. Rehn, M., Veikkola, T., Kukk-Valdre, E., Nakamura, H., Ilmonen, M., Lombardo, C., Pihlajaniemi, T., Alitalo, K., and Vuori, K. (2001) Interaction of endostatin with integrins implicated in angiogenesis, *Proc. Natl. Acad. Sci. U.S.A. 98*, 1024−1029.
53. Dixelius, J., Larsson, H., Sasaki, T., Holmqvist, K., Lu, L., Engstrom, A., Timpl, R., Welsh, M., and Claesson-Welsh, L. (2000) Endostatin-induced tyrosine kinase signaling through the Shb adaptor protein regulates endothelial cell apoptosis, *Blood 95*, 3403−3411.
54. Mellman. I., Fuchs. R., and Helenius. A. (1986) Acidification of the endocytic and exocytic pathways, *Annu. Rev. Biochem. 55*, 663−700.

BI0357863